

Overall water splitting on tungsten-based photocatalysts with defect pyrochlore structure

Shigeru Ikeda^{1,2,*}, Tomokazu Itani¹, Keigo Nango¹, and Michio Matsumura¹

¹Research Center for Solar Energy Chemistry, Osaka University, 1-3 Machikaneyama, Toyonaka, Osaka 560-8531, Japan

²“Conversion and Control by Advanced Chemistry”, PRESTO, Japan Science and Technology Agency (JST), 4-1-8 Honcho, Kawaguchi, Saitama 332-0012, Japan

Received 3 June 2004; accepted 27 August 2004

Defect pyrochlore-type oxides, AMWO_6 ($A = \text{Rb, Cs}$; $M = \text{Nb, Ta}$), loaded with nickel oxide showed photocatalytic activity for overall water splitting under ultraviolet-light irradiation. The conduction bands of the materials are thought to be composed of the W5d orbital hybridized with the Nb5d or Ta4d orbital.

KEY WORDS: photocatalysis, overall water splitting, defect pyrochlore-type oxide, tungsten, conduction band.

1. Introduction

Since the discovery of photoelectrochemical water splitting at a semiconductor surface [1], photoinduced water decomposition into hydrogen (H_2) and oxygen (O_2) in a stoichiometric ratio has been a most significant research objective for chemists. It has been suggested [2] that one of the indispensable properties required for semiconductor materials to drive the reaction is that the valence and the conduction bands have appropriate potential, i.e., the valence band is more positive than the oxidation potential of water to form O_2 and the conduction band is more negative than the reduction potential of water to form H_2 . There are also other reaction and transport step included in the photocatalytic water splitting on semiconductor particles, such as photoexcitation to generate electrons (e^-) and holes (h^+), migration of them to the surfaces of particles, reduction and oxidation of surface-adsorbed water by them to produce H_2 and O_2 , respectively, and desorption of H_2 and O_2 from the surface of the photocatalyst. Reaction kinetics must also be sufficient for practical applications. Due to the difficulty in meeting all of these requirements using conventional materials, new materials have been synthesized and examined for the purpose of photocatalytic water splitting. Some photocatalysts with wide band gaps have been found to be active for water splitting into H_2 and O_2 in stoichiometric amounts under ultraviolet (UV)-light irradiation [3–13]. Although the final goal of photocatalytic overall splitting is utilization of sunlight, i.e., having a visible-light response, with high efficiency, materials that work even under UV irradiation are still limited and photon

energy conversion is far from the stage of practical use at present. Thus, it is important to develop a new class of photocatalyst materials.

We examined various kinds of materials and found that some tungsten-containing oxides that have a defect pyrochlore-type crystalline structure with the general formula of AMWO_6 ($A = \text{Rb, Cs}$; $M = \text{Nb, Ta}$) show activity for the overall water splitting under UV-light irradiation. Here, we report activities of these photocatalysts in conjunction with their optical properties and structural characteristics.

2. Experimental

Polycrystalline AMWO_6 ($A = \text{Rb, Cs}$; $M = \text{Nb, Ta}$) powders were synthesized by calcining powder mixtures of carbonates (A_2CO_3 , $A = \text{Rb, Cs}$), oxides (M_2O_5 , $M = \text{Nb, Ta}$), and WO_3 at 1273 K for 10 h in air. The molar ratio among A, M, and W in the starting materials was 1.05:1:1; a slight excess of carbonates was necessary to compensate the volatilization of the alkaline metals during calcination. After the calcination, white powders thus obtained were washed with distilled water to eliminate excess alkaline metal ions and dried at 353 K at ambient pressure. Onto the as-prepared compounds of AMWO_6 ($A = \text{Rb, Cs}$; $M = \text{Nb, Ta}$), nickel (Ni) was impregnated from an aqueous solution of nickel nitrate ($\text{Ni}(\text{NO}_3)_2$). The Ni-impregnated samples were submitted to reduction in a stream of H_2 (26.7 kPa) at 750 K for 2 h and subsequently to oxidation in a stream of O_2 (13.3 kPa) at 473 K for 1 h. By this treatment, the loaded Ni was partially oxidized (NiO_x), being an active catalyst for reduction of water [6]; the pretreatment is indispensable for the present materials to induce overall water splitting. The amount

*To whom correspondence should be addressed.

E-mail: siked@chem.es.osaka-u.ac.jp

of loaded NiO_x on all of the materials was fixed at 1.0 wt%.

The crystallographic structure of the synthesized materials was confirmed by X-ray diffraction using a Rigaku MiniFlex X-ray diffractometer ($\text{CuK}\alpha$, Ni filter). Ultraviolet and visible-light diffuse reflection (DR) spectra were obtained by using a Simadzu UV-2450 UV-VIS spectrometer equipped with an integrating sphere, and the data were converted to Kubelka-Munk (KM) function. BET surface areas were measured by nitrogen (N_2) adsorption at 77 K using a Quantachrome AUTOSORB-1 automated gas sorption system after drying at 573 K for 3 h under vacuum.

Photocatalytic reaction was performed in an air-free closed gas circulation system with a quartz reaction cell. Aqueous suspensions composed of 300 mg NiO_x -loaded AMWO_6 ($\text{NiO}_x/\text{AMWO}_6$) and a 70 cm^3 aqueous alkaline metal hydroxide (AOH ($\text{A} = \text{Rb}$, Cs)) solution (1.0 mol dm^{-3}) were photoirradiated by a 1 kW super-pressure mercury (Hg) lamp (Ushio) from the side of the reaction cell under Ar (30 kPa) with magnetic stirring. The apparent quantum yield, defined as molar ratio of the product (twice the molar amount of H_2) to the incident photons, was determined at a wavelength of 313 nm. This monochromatic light was selected from the light beam of an Hg lamp using a band pass filter (ASAHI SPECTRA CO. HG-313), and the incident photon flux was determined using an Ushio USR-40V/D spectra radiometer. The amounts of H_2 and O_2 evolved were determined using a Shimadzu GC-8A gas chromatograph equipped with an MS-5A column (GL Sciences) and a TCD detector through a gas sampler (3 cm^3) that was directly connected to the reaction system to prevent any contamination from air [6].

3. Results and discussion

Figure 1 shows the schematic structure of defect pyrochlore-type oxides having the formula of AMWO_6 ($\text{A} = \text{Rb}$, Cs ; $\text{M} = \text{Nb}$, Ta). The structure is a rigid three-dimensional framework consisting of corner-sharing MO_6 - and WO_6 -octahedra, forming parallel tunnels each with a hexagonal cross section. Both M and W ions are considered to be distributed randomly in the framework. RbNbWO_6 has almost the same lattice parameters as those of RbTaWO_6 , and CsNbWO_6 has almost the same lattice parameters as those of CsTaWO_6 [14–16]. Alkaline metal ions (A^+) occupy the tunnels coordinating to six oxygen atoms on the MO_6 - and WO_6 -octahedra. It has been reported that various kinds of monovalent cations such as Na^+ , K^+ , H^+ , and NH_4^+ can be replaced instead of the A^+ ions of the AMWO_6 compounds; their lattice positions are altered depending on their ionic radii [16]. Owing to the relatively large ionic radii of both rubidium (Rb) and

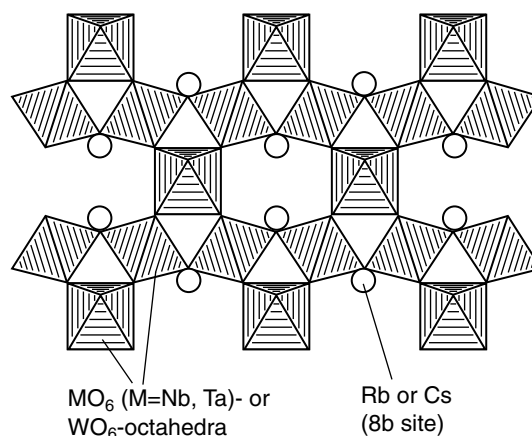


Figure 1. Schematic structure of a $\{110\}$ face of $\text{Rb}(\text{Cs})\text{MWO}_6$ ($\text{M} = \text{Nb}$, Ta) with a defect pyrochlore-structure.

cesium (Cs) ions used in the present study, both of them are known to occupy the same site (8b site) [14,15]. Therefore, the series of materials employed here are considered to have almost the same crystalline structure.

Figure 2 shows DR spectra of AMWO_6 ($\text{A} = \text{Rb}$, Cs ; $\text{M} = \text{Nb}$, Ta). Both of the niobium (Nb)-containing materials (ANbWO_6) show photoabsorption onset at ca. 340 nm in the UV region. Similarly, both of the tantalum (Ta)-containing compounds (ATaWO_6) exhibited almost the same spectra, whose absorption edges are ca. 330 nm. These results suggest that the effect of the alkaline metal ions on the band structure is not significant in the present system. The similarity between the optical properties of the material with Rb and the

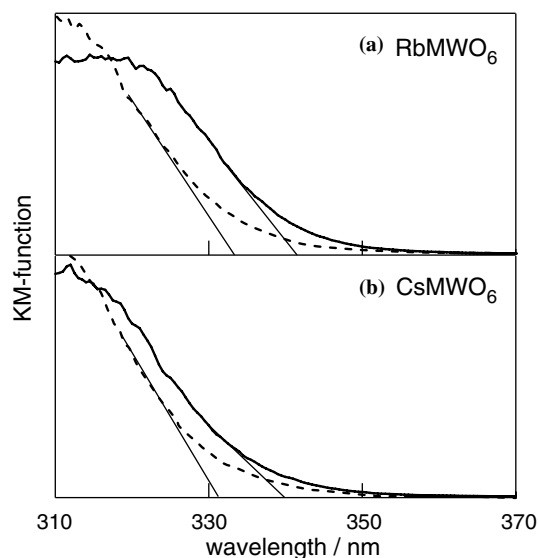


Figure 2. DR spectra of (a) RbMWO_6 and (b) CsMWO_6 . Solid and dotted lines represent the samples with $\text{M} = \text{Nb}$ and $\text{M} = \text{Ta}$, respectively. Photoabsorption edges and band gaps of these materials were determined by extrapolating the linear regions of the spectra as shown in the figures.

material with Cs is thought to arise from this structural similarity, as discussed above. On the other hand, replacement of Nb with Ta results in a small shift (less than 10 nm) of the photoabsorption edge toward a shorter wavelength. It has also been reported in other series of photocatalytic materials such as $\text{Sr}_2\text{M}_2\text{O}_7$ and AgMO_3 ($\text{M} = \text{Nb, Ta}$) that the absorption edge is shifted toward a shorter wavelength by replacing Nb with Ta [7,8,13]. In these cases, shifts of 50–75 nm have been reported and are attributed to the relatively negative energy levels of the Ta5d orbital compared to those of the Nb4d orbital, which contribute to the bottom of conduction bands of these materials. Compared with these previous systems, it is clear that the shifts observed in the present AMWO_6 compounds are quite small. Although there is no experimental and theoretical information available at present, these results and facts suggest that the contribution from Nb4d and/or Ta5d to the bottom of the conduction band is rather small (see below).

Figure 3 shows representative time course curves of liberation of H_2 and O_2 on $\text{NiO}_x/\text{RbTaWO}_6$ suspended in an aqueous RbOH solution (1.0 mol dm^{-3}) under UV light irradiation. The reaction system was evacuated at 11-h intervals. In each run, monotonical accumulation of H_2 and O_2 in a stoichiometric ratio ($\text{H}_2:\text{O}_2 = 2:1$) was observed, though the rates of H_2 and O_2 liberation decreased slightly with successive runs. The total amounts of evolved H_2 and O_2 during irradiation for 44 h reached 2.5 and 1.3 mmol, respectively, while the amount of RbTaWO_6 used in the experiment was 0.55 mmol; the much larger amounts of evolved H_2 and O_2 than the amount of RbTaWO_6 are consistent with the premise that the reaction proceeds photocatalytically. XRD patterns before and after the reaction (figure 4) revealed that the crystal structure was essentially maintained after the reaction for 44 h, i.e., the gradual decrease in the activity was not due to the instability of the material. However, the gray color of the particles of $\text{NiO}_x/\text{RbTaWO}_6$, attributed to the photoabsorption of NiO_x deposits, faded to some extent after the reaction. This finding suggests that the decrease in the activity is due to the collapse of the loaded NiO_x catalyst by elution and/or alteration of the oxidation state. It is also noted that the addition of RbOH to the reaction solution is indispensable to induce stoichiometric H_2 and O_2 liberation. From the fact that a suspension of $\text{NiO}_x/\text{RbTaWO}_6$ powders in pure water showed a pH of ca. 9.5, elution of Rb ions from the crystal lattice accompanied by insertion of protons (H^+) or hydronium ions (H_3O^+) was expected without the addition of RbOH . These H^+ and H_3O^+ species might be trap sites acting as recombination centers of photo-excited e^- and h^+ . Actually, the protonated form, HMWO_6 ($\text{M} = \text{Nb, Ta}$), prepared by ion-exchange of RbMWO_6 ($\text{M} = \text{Nb, Ta}$) in 3 mol dm^{-3} HNO_3 solution for 20 days at 333 K [16], loaded with NiO_x did not

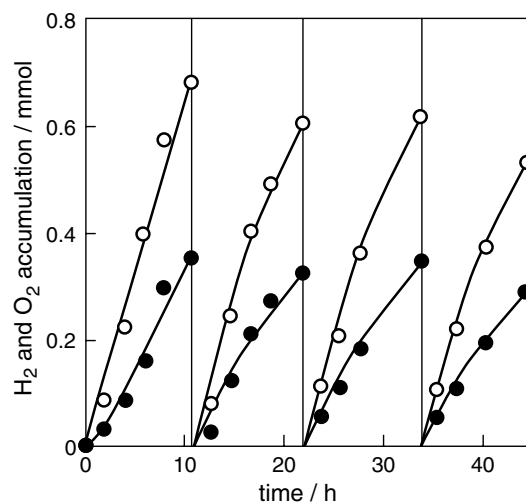


Figure 3. Photocatalytic water splitting over $\text{NiO}_x/\text{RbTaWO}_6$ in an aqueous solution of RbOH (1.0 mol dm^{-3}) under UV light irradiation. Open and filled circles denote the accumulation of H_2 and O_2 , respectively.

show activity for overall water splitting. The high concentration of Rb ions in the solution may suppress their elution from the lattice and allow the maintenance of photocatalytic activity.

Similar to the case of the $\text{NiO}_x/\text{RbTaWO}_6$ photocatalyst, stoichiometric H_2 and O_2 liberation was observed on all of the $\text{NiO}_x/\text{AMWO}_6$ ($\text{A} = \text{K, Rb, Cs}$; $\text{M} = \text{Nb, Ta}$) catalysts used in the present study. Table 1 summarizes the rates of H_2 and O_2 evolution on these catalysts by considering the initial 3 h of irradiation. Band gap energies estimated from the onset wavelengths of DR spectra shown in figure 2 and BET surface areas of these materials are also summarized in this table. Since the rates were not changed when a larger amount of photocatalysts (500 mg) was used, observed rates were maximum activity for all of the photocatalysts in the present conditions, though other parameters, e.g., alkaline concentration and amount of loaded NiO_x ,

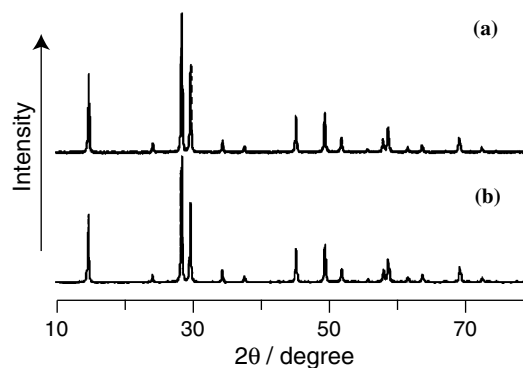


Figure 4. XRD patterns of $\text{NiO}_x/\text{RbTaWO}_6$ (a) before and (b) after photoirradiation.

Table 1
Photocatalytic water splitting over AMWO₆ (A = Rb, Cs) loaded with NiO_x

Catalyst	R _{H₂} ^b / μmol h ⁻¹	R _{O₂} ^c / μmol h ⁻¹	b.g. ^d /eV	S ^e / m ² g ⁻¹
RbNbWO ₆	11.4	4.3	3.6	2.7
RbTaWO ₆	69.7	34.5	3.8	3.0
CsNbWO ₆	10.1	4.7	3.6	2.9
CsTaWO ₆	19.7	8.8	3.8	3.2

^acatalyst (300 mg) was suspended in 1.0 mol dm⁻³ of aqueous AOH (A = Rb, Cs) solution (70 cm³) and photoirradiated with 1 kW of ultra-high pressure Hg lamp under Ar (30 kPa).

^bRate of H₂ liberation.

^cRate of O₂ liberation.

^dDenotes band gap energy determined from onsets of the photoabsorption shown in figure 2.

^eDenotes BET surface area.

were not optimized. Moreover, from the fact that there is no significant difference in BET surface area between samples, i.e., these samples have almost the same particle sizes, the observed differences in activity are not dominated by such physicochemical properties. Thus, it can be deduced from the results that Ta-containing materials show higher levels of activity than do Nb-containing materials mainly due to the difference in their band structures. As previously reported by Scaife [17], the energy levels of the top of valence bands of oxide semiconductors composed of transition metals of d(0) configuration are almost the same (2.9 V vs. NHE) because their valence bands consist of O2p orbitals. On the basis of this understanding, it is thought that Ta-containing materials have more negative conduction band energy levels (−0.9 V vs. NHE) than do Nb-containing materials (−0.7 V vs. NHE) because the former have larger band gap energies than those of the latter, as shown in figure 5. Therefore, the higher levels of activity of the Ta-containing materials might be due to their negative potential of conduction bands. Due to the similar crystalline structures and optical properties, it is reasonable to assume that there is no significant

difference between the activity of RbNbWO₆ and CsNbWO₆. On the other hand, RbTaWO₆ showed a higher level of activity than that of CsTaWO₆. This difference cannot be explained in terms of band energies. Results of further characterization of these materials will be presented elsewhere.

One of the notable features of the present materials is that the W5d orbital is thought to contribute to the conduction band, as mentioned above. It is well known that the bottom of a conduction band made from a W5d orbital in a binary system, WO₃, is more positive than the reduction potential of water into H₂ (+0.36 V vs. NHE, see Figure 5) [18], and water splitting therefore does not occur. Thus, the W5d orbital in the case of the present AMWO₆ (A = K, Rb, Cs; M = Nb, Ta) materials might contribute to the conduction band, presumably through hybridization with the Ta5d and Nb4d orbitals. For the present Ta-containing photocatalysts, the band gap energies were smaller than the reported highly active photocatalysts based on tantalates that have band gap energies of more than 4.0 eV [7, 8, 13]. This suggests that hybridization with a W5d orbital is an effective means for lowering the energy level of the conduction bands of Ta-based materials. The apparent quantum yield of water splitting on NiO_x/RbTaWO₆, which showed the highest level of activity, was determined to be 0.015 under irradiation at a wavelength of 313 nm. Compared to previously reported tantalates [7, 8, 13], this value is small by one order of magnitude. The smaller band gap of ca. 3.8 eV leading to lower reduction ability to produce H₂ might account for this slower rate.

We also found that the Nb-containing materials are capable of splitting water even though their activity levels are lower than those of the Ta-containing materials. With the exception of a few Nb-based photocatalysts [5–7] and some mixed oxides based on Zn(II), Ga(III), In(III), Ge(IV), and Sb(V) with d(10) configuration [9], most of the materials that are able to drive overall water splitting contain Ta or titanium (Ti) as chief components. Hence, this finding may give an alternative approach for designing new photocatalytic materials.

In conclusion, we have found a new class of photocatalysts for overall water splitting under UV-light irradiation. It has been demonstrated that the conduction band energies can be tuned by mixing the appropriate elements. However, since valence bands of the present oxide photocatalysts consist of O2p orbitals and their potentials (2.9 V vs. NHE) are considerably more positive than the oxidation potential of water to form O₂ (1.23 V vs. NHE) as in the case of previous photocatalysts for overall water splitting, the band gap is inevitably larger than ca. 3 eV and thereby the oxide photocatalyst responds only to UV light. Therefore, a valence band of which the potential is more negative than that consisting of O2p orbitals has to be formed with some other orbitals for capturing sunlight radiation. Along with this strategy, further studies and design of photocatalytic materials are now underway.

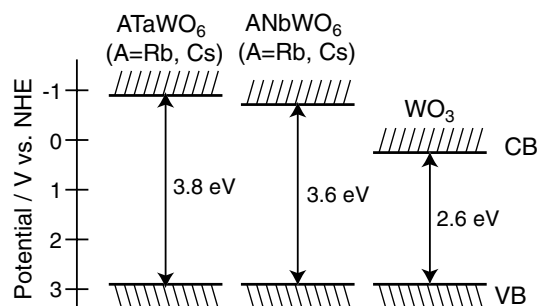


Figure 5. Possible band structures of Rb(Cs)MWO₆ (M = Nb, Ta) and WO₃.

Acknowledgements

This study was partly supported by the Research Institute of Innovative Technology for the Earth (RITE). We thank Prof Akihiko Kudo (Science University of Tokyo) for his stimulating suggestions and discussion.

References

- [1] A. Fujishima and K. Honda, *Nature* 238 (1972) 37.
- [2] H. Gerischer, *J. Electroanal. Chem.* 82 (1977) 133.
- [3] J.M. Lehn, J.-P. Sauvage and R. Ziessel, *Nouv. J. Chem.* 4 (1980) 623.
- [4] K. Sayama and A. Arakawa, *J. Photochem. Photobiol. A Chem.* 77 (1994) 243.
- [5] H.G. Kim, D.W. Hwang, J. Kim, Y.G. Kim and J.S. Lee, *Chem. Commun.* (1999) 1077.
- [6] K. Domen, J.N. Kondo, M. Hara and T. Takata, *Bull. Chem. Soc. Jpn.* 73 (2000) 1307, and references therein.
- [7] A. Kudo, H. Kato and S. Nakagawa, *J. Phys. Chem. B* 104 (2000) 571.
- [8] H. Kato, H. Kobayashi and A. Kudo, *J. Phys. Chem. B* 106 (2002) 12441.
- [9] J. Sato, N. Saito, H. Nishiyama and Y. Inoue, *J. Phys. Chem. B* 107 (2003) 7965, and references therein.
- [10] H. Kato and A. Kudo, *Catal. Today* 78 (2003) 561.
- [11] M. Machida, K. Miyazaki, S. Matsushima and M. Arai, *J. Mater. Chem.* 13 (2003) 1433.
- [12] R. Abe, M. Higashi, Z. Zou, K. Sayama, Y. Abe and H. Arakawa, *J. Phys. Chem. B* 108 (2004) 811.
- [13] A. Kudo, *Catal. Surv. Asia* 7 (2003) 31.
- [14] T. Kar and R.N.P. Choudhary, *Mater. Sci. Eng. B90* (2002) 224.
- [15] R.W. Specht, D.G. Brunner and G. Tomandl, *Adv. Ceram. Mater.* 2 (1987) 789.
- [16] P.W. Barnes, P.M. Woodward, Y. Lee, T. Vogt and J.A. Hriljac, *J. Am. Chem. Soc.* 125 (2003) 4572.
- [17] D.E. Scaife, *Solar Energy* 25 (1980) 41.
- [18] M.A. Butler, *J. Appl. Phys.* 48 (1977) 1914.